Backbone Stretching of Wormlike Carbosilane Dendrimers

Nadjet Ouali,† Stéphane Méry,* and Antoine Skoulios

Groupe des Matériaux Organiques, Institut de Physique et Chimie des Matériaux de Strasbourg, 23 rue du Loess, 67037 Strasbourg Cedex, France

Laurence Noirez

Laboratoire Léon Brillouin (CEA-CNRS), C.E.-Saclay, 91191 Gif sur Yvette Cedex, France

Received February 23, 2000; Revised Manuscript Received June 1, 2000

ABSTRACT: Wormlike dendrimers made of flexible and noninteracting segments were synthesized. Starting from a poly(methylhydrosiloxane) $\mathbf{G_0}$ and using short propylsilane branches, the synthesis did not go beyond the second generation, as predicted from steric congestion. The starting polymer and the $\mathbf{G_1}$ and $\mathbf{G_2}$ dendrimers synthesized were studied by small-angle neutron scattering. The molecular-weight dependence of their radius of gyration ($R_g \propto M^\nu$, ν growing from 0.53 for $\mathbf{G_0}$ to 0.94 for $\mathbf{G_2}$) showed the backbone conformation to go from very flexible for $\mathbf{G_0}$ to nearly rodlike for $\mathbf{G_2}$. This was supported by the growth of the persistence length from 12 to over 200 Å, as deduced from an analysis of the data according to Benoît−Doty's law. The dendrimers being made of flexible parts, their stretching was attributed to the congestion of the peripheral branches. The absence of liquid crystallinity was imputed to the dynamical flexibility of the molecules.

I. Introduction

Ball-like dendrimers are nanomaterials formed by multiplicative growth from a central polyfunctional core and presenting an orderly, highly symmetrical branched structure.[1,2] After successive generations of branches, their growth is limited by surface congestion.[3] Recently, the synthesis of wormlike dendrimers (referred to by other authors as rodlike, linear, cylindrical, or dendronized polymers) has become an increasingly attractive scientific goal.[4] In such dendrimers, the branches do not emanate from a single core as in ball-like dendrimers, but from a sequence of sites distributed along a polymer backbone. Depending on the backbone stiffness, the branch size, and the degree of coverage, their overall shape is no longer spherical but tends to become cylindrical as sketched in Figure 1. They can be synthesized following either a divergent approach, by stepwise grafting successive generations of branches onto a multifunctional linear polymer,[5,6] or a convergent strategy, by attaching prefabricated dendrons directly onto a reactive polymer chain.[7−10] They can also be synthesized by using classical polycondensation or polymerization of prefabricated dendrons.[11−21]

Generally made of aromatic segments and polar groups, the wormlike dendrimers reported in the literature are of course subject to strong inter-dendron interactions liable to enhance rigidity. Some of them, adsorbed on graphite and visualized by scanning force microscopy (SFM), appeared as nanorods tending to align parallel to each other.[17,22−24] In the special case of the branched polymers studied by Percec et al.,[15−17,22] all terminated by long paraffin chains, the molecular morphology was found to change with the backbone length due to steric congestion, starting from spherical and ending in cylindrical particles. It is of interest to note that these polymers were in addition found to form liquid crystals of cubic or columnar symmetry, probably due to amphiphilicity and microphase segregation.

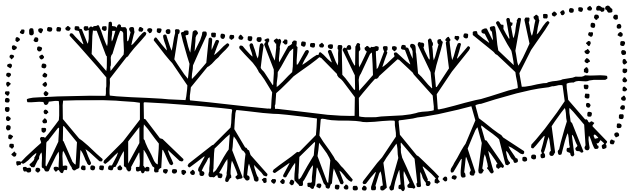

Figure 1. Schematic representation of a wormlike dendrimer.

The statistics of conformation of wormlike dendrimers was not investigated until quite recently. In a first study by Schlüter et al.,[11] using size exclusion chromatography (SEC) combined with static and dynamic light-scattering, a polystyrene with second-generation Fréchet-type dendrons was found to behave like a Gaussian rather than a wormlike chain. In a more recent study by Percec et al.,[22] carried out by SEC combined with light scattering, the dendrimers were on the contrary found to be considerably elongated. With a polymethacrylate backbone bearing sterically demanding dendrons, the length of the molecules compared well with that measured by SFM, corresponding to a maximum stretching of the backbone by the steric repulsion of the bulky side chains, whereas with a polystyrene backbone carrying less branched dendrons, the length was two times shorter than expected, suggesting a disordered helixlike conformation. Finally, in a series of small-angle neutron-scattering (SANS) experiments performed with polystyrene dendrimers made of Fréchet dendrons,[23,25] Schlüter et al. analyzed the intermediate and asymptotic parts of the scattering curves, concluding that the statistical Kuhn segment length initially increases in proportion to the chain diameter and then to a greater degree due to steric overcrowding. It is well to specify in this connection that, in agreement with Percec's interpretation, the dendrimer molecules never attain full extension, because high generation dendrons force

* Author for correspondence. E-mail: stephane.mery@ipcms.u-strasbg.fr.

† Ph.D. Thesis, Louis-Pasteur University of Strasbourg, December 1998.

10.1021/ma000327k CCC: $19.00
Published on Web 07/18/2000

the polymer backbone out of its all-trans conformation, (probably) leading to helical coiling.

The present paper deals with the synthesis of new wormlike dendrimers obtained by grafting propylsilane branches onto linear siloxane chains, both species being intrinsically flexible and essentially inert with regard to interactions. The idea was to check whether steric overcrowding alone was apt to affect the conformation of wormlike dendrimers and induce the stretching of backbones until rodlike particles are formed. To maximize the steric effect of overcrowding and reach congestion as early as possible, propylsilane branches were chosen for their shortness and their ability to initiate dense branching. In a second part, the present paper deals with the conformational properties of such dendrimers in solution, as deduced from SANS experiments. Instead of analyzing as usually the shape of the intermediate and asymptotic parts of the scattering curves, which is not always an easy task, attention was focused on the Guinier small-angle region which contains information about molecular weights and radii of gyration. Several sharp fractions of the starting poly(methylhydrosiloxane) and of each dendrimer synthesized were, of course, studied in order to determine the molecular weight dependence of the radius of gyration and the evolution of the persistence length with the degree of branching. Finally, the thermal and structural properties of the dendrimers were investigated by differential scanning calorimetry, polarizing optical microscopy, and X-ray diffraction.

II. Experimental Section

A. Techniques. The molecular weight and molecular-weight distribution of the starting poly(methylhydrosiloxane) were determined by SEC in toluene. The Waters chromatograph used was equipped with a set of three (one 500 Å and two mixed-B) PL gel columns and a Shimadzu (RID-6A) differential refractometer. It was calibrated with poly(dimethylsiloxane) standards.

The molecular weight and molecular-weight distribution of the dendrimers was determined by SEC in tetrahydrofuran (THF). The Waters chromatograph used was equipped with a set of five (10^5 and 10^4 Å and three mixed-B) PL gel columns and a Shimadzu (RID-6A) differential refractometer. It was calibrated with polystyrene standards.

Synthesized dendrimers were isolated by preparative SEC in THF. The Waters chromatograph used was equipped with a series of Ultrastyragel columns (linear mixed-bed and 10^4 and 10^3 Å) and a Waters (R401) differential refractometer. It was calibrated with polystyrene standards.

^{1}H and ^{13}C NMR spectra were recorded using a Bruker AC-200F spectrometer (at 200 and 50 MHz, respectively). IR measurements were carried out with a Bomem MB 155 spectrometer. Glass transitions were detected with a Perkin-Elmer DSC-7 instrument at a heating rate of 10 °C/min. SANS measurements were performed at Léon-Brillouin Laboratory in CEA-Saclay, France (Orphée reactor, PACE spectrometer). X-ray diffraction studies were carried out using a Guinier focusing camera equipped with a bent-quartz monochromator (Cu Kα_1 radiation), a modified INSTEC heating sample-holder, and an Inel CPS 120 curved position-sensitive detector. Optical microscopy observations were made with a polarizing Leitz-Wetzlar microscope equipped with a Mettler FP82 hot stage.

B. Materials. Trimethylsilyl terminated poly(methylhydrosiloxane) (noted in the following as **G_0**) was purchased from Petrarch System Inc. (PS122, given for M_n = 4500−5000). Before use, it was characterized by SEC (Figure 2): M_n = 4700 ± 450; M_w/M_n = 2.8. It proved to contain 5−8% w/w of cyclic oligomers. Its degree of polymerization (number of silicon atoms in the polymer chains) was DP_n = 78 ± 7. It was used as received, the cyclic oligomers being eliminated by SEC during the isolation of the first generation of dendrimers.

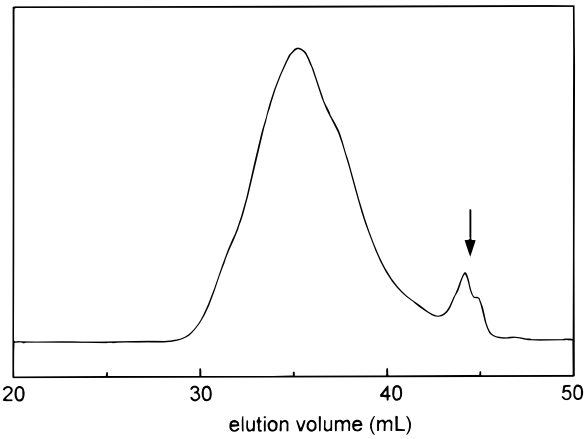

Figure 2. Size-exclusion-chromatography graph of the crude starting poly(methylhydrosiloxane) **G_0** polymer. Arrow shows the presence of (cyclic) oligomers.

Diethyl ether (dried over $CaCl_2$) and benzene (anhydrous grade) were distilled over Na, while tetrahydrofuran (dried over KOH) was distilled over $LiAlH_4$; before use, all of them were stored in an argon atmosphere. Allyltrichlorosilane and trichlorosilane (Gelest Inc.) were distilled over quinoleine in argon atmosphere into a dropping funnel sealed to the reactor. The Karstedt catalyst (divinyltetramethyldisiloxane−platinum (0) complex 3−3.5% w/w in xylene) was purchased from Gelest Inc. and used as received. The Grignard reagents were prepared using Mg turnings (99.8%) from Fluka and freshly distilled allyl bromide (99%) from Aldrich. The trimethylsilylation solution was prepared from 1,1,1,3,3,3-hexamethyldisilazane (99.9%), chlorotrimethylsilane (99+%), and high-quality-grade triethylamine (99%), used as received from Aldrich.

C. Syntheses. The dendrimers were synthesized as outlined in Scheme 1, using hydrosilylation and alkylation reactions. To minimize coupling side reactions (due to the presence of silanol groups resulting from the hydrolysis of possibly non-alkylated chlorosilane groups), dendrimers were submitted to trimethylsilylation[26] before isolation. All experiments were carried out in argon atmosphere, and much care was taken to avoid any trace of humidity. Most parts of the glassware used were sealed together, flamed with a torch under vacuum, and purged with argon several times prior to use.

1. Synthesis of G1. Dissolved in anhydrous benzene (50 mL), the starting polymer **G_0** (6.0 g, 0.10 mol of SiH) was introduced into the reactor, freeze-dried, and redissolved in anhydrous benzene (60 mL). Allyltrichlorosilane (2-fold excess, 45 mL, 0.30 mol), freshly distilled over quinoleine into a dropping funnel sealed to the reactor, was then added along with the Karstedt catalyst (270 μL, 500 ppm/SiH). The mixture was heated at 70 °C for 48 h under stirring. The unreacted allyltrichlorosilane and most of the solvent were removed by evaporation under reduced pressure, leaving a highly concentrated benzene solution of the intermediate **G_0Cl** product.

Freshly prepared allylmagnesium bromide (2 equiv/SiCl), dissolved in diethyl ether (700 mL), was added dropwise to the concentrated benzene solution of **G_0Cl** previously cooled to 0 °C (ice/water bath). After refluxing at 40 °C for 48 h, the mixture was cooled back to 0 °C and hydrolyzed by pouring into a vigorously stirred 10% acetic acid/sodium acetate buffer solution (pK_a = 4.8) (700 mL). The ether layer was extracted, washed with a saturated aqueous solution of $NaHCO_3$ (500 mL), then with pure water (3 × 500 mL).

To protect silanol groups eventually formed during the washing process with water, the solution, dried over $MgSO_4$ and filtered off, was submitted to trimethylsilylation.[26] Added with a dry diethyl ether solution (60 mL) of triethylamine (42 mL, 0.30 mol), 1,1,1,3,3,3-hexamethyldisilazane (31.8 mL, 0.15 mol) and chlorotrimethylsilane (15 mL, 0.12 mol), it was stirred at room temperature under argon atmosphere for 24

Scheme 1. Synthesis of the Dendrimers

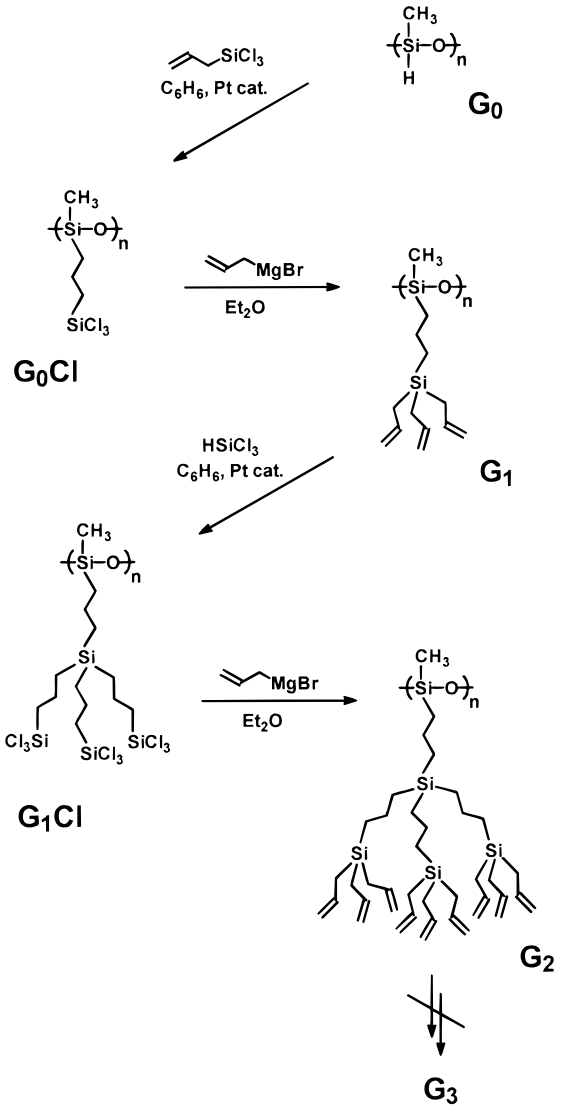

h. After addition of water (500 mL), the ether layer was extracted, washed with water (5 × 500 mL), dried over $MgSO_4$, filtered through a 0.47 μm pore-size filter, and evaporated to dryness.

Using preparative SEC in THF, the expected dendrimer **G_1** was finally isolated from the crude residue as a colorless, thick oil (60% yield). It was characterized by analytical SEC [THF, polystyrene standards, $M_n = 6200$, $M_w/M_n = 1.2$], ^{1}H NMR [($CDCl_3$, ppm) δ 0.10 (s, 3.2H, $-Si-CH_3$), 0.65 (m, 4H, $-Si-CH_2-$), 1.43 (m, 2H, $-CH_2-$), 1.60 (d, 6H, $-Si-CH_2-$), 4.90 (t, 6H, $=CH_2$), 5.80 (m, 3H, $=CH-$)], ^{13}C NMR [($CDCl_3$, ppm) δ 0.0 ($-Si-CH_3$), 16 ($-Si-CH_2-$), 17 ($-CH_2-$), 20 ($-Si-CH_2-$), 114 ($=CH_2$), 134 ($=CH-$)], IR [(KBr, cm^{-1}) ν_{max} 1022 ($-Si-O-Si-$), 1258 ($-Si-CH_3$), 1630 ($-C=C-$), 2916 ($-CH_2-$)], elemental analysis [Anal. Found (Calcd for $(C_{13}H_{24}OSi_2)_n$): C, 61.31 (61.70); H, 9.63 (9.59); Si, 22.50 (22.34)], and titration of allylic double bonds[27] [found (calculated for 100% substitution): 14.36% (14.29%)]. The absence of an IR peak at 2166 cm^{-1} (ν_{Si-H}) and a ^{1}H NMR peak at 4.75 ppm (Si−H) suggest that the alkylation reaction was complete. The rate of substitution determined by ^{1}H NMR, elemental analysis, and titration of double bonds was 100% with an accuracy of 10, 5, and 10%, respectively.

2. Synthesis of G2. Dissolved in anhydrous benzene (20 mL), dendrimer **G_1** (1.4 g, 16.7 mmol of allylic groups), was introduced into the reactor, freeze-dried, and redissolved in anhydrous benzene (40 mL). Trichlorosilane (large excess, 17 mL, 0.168 mol), freshly distilled over quinoleine into a dropping funnel sealed to the reactor, was then added along with the Karsdedt catalyst (67 μL, 750 ppm/allylic groups). The mixture was heated at 70 °C for 72 h under stirring, then submitted to slow evaporation under reduced pressure to remove unreacted trichlorosilane and most of the solvent, leaving a highly concentrated benzene solution of the intermediate **G_1Cl** product.

Freshly prepared allylmagnesium bromide (6 equiv/SiCl) dissolved in diethyl ether (700 mL) was added dropwise to the concentrated benzene solution of **G_1Cl** previously cooled to 0 °C (ice/water bath). After refluxing at 40 °C for 92 h, the mixture was cooled back to 0 °C and hydrolyzed by pouring into a vigorously stirred 10% acetic acid/sodium acetate buffer solution (700 mL). The ether layer was extracted, then washed with a saturated aqueous solution of $NaHCO_3$ (500 mL) and pure water (3 × 500 mL).

To protect silanol groups eventually formed during the washing process with water, the solution, dried over $MgSO_4$ and filtered off, was submitted to trimethylsilylation.[26] Added to a dry diethyl ether solution (10 mL) of triethylamine (7 mL, 0.05 mol), 1,1,1,3,3,3-hexamethyldisilazane (5.3 mL, 0.025 mol) and chlorotrimethylsilane (2.5 mL, 0.02 mol), it was stirred at room temperature under argon atmosphere for 24 h. After addition of water (500 mL), the ether layer was extracted, washed with water (5 × 500 mL), dried over $MgSO_4$, filtered through a 0.47 μm pore-size filter, and evaporated to dryness.

Using preparative SEC in THF, the expected dendrimer **G_2** was finally isolated from the crude residue as a white, waxy paste (50% yield). It was characterized by analytical SEC [THF, polystyrene standards, $M_n = 30\,500$, $M_w/M_n = 1.6$], ^{1}H NMR [($CDCl_3$, ppm) δ 0.08 (b, 3.2H, $-Si-CH_3$), 0.62 (b, 8H, $-Si-CH_2-$), 1.26 (b, 16H, $-CH_2-$), 1.61 (d, 18H, $-Si-CH_2-$), 4.90 (t, 18H, $=CH_2$), 5.80 (m, 9H, $=CH-$)], ^{13}C NMR [($CDCl_3$, ppm) δ 0.0 ($-Si-CH_3$), 17 ($-Si-CH_2-$), 19 ($-CH_2-$), 20 ($-Si-CH_2-$), 114 ($=CH_2$), 135 ($=CH-$)], IR [(KBr, cm^{-1}) ν_{max} 1021 ($-Si-O-Si-$), 1257 ($-Si-CH_3$), 1629 ($-C=C-$), 2914 ($-CH_2-$)], elemental analysis [Anal. Found (Calcd for $(C_{40}H_{72}OSi_5)_n$): C, 66.05 (67.66); H, 10.17 (10.23); Si 20.82 (19.83)], and titration of allylic double bonds [found (calculated for 100% substitution): 12.74% (15.22%)]. The rate of substitution determined by ^{1}H NMR, elemental analysis, and titration of double bonds[27] was 85 ± 8%, 80% ± 4%, and 84% ± 8%, respectively.

D. Small-Angle Neutron Scattering. Two different spectrometer configurations were used: for dendrimers **G_0** and **G_1**, the beam wavelength was $\lambda = 6$ Å with a sample to detector distance of $D = 1.5$ m; for dendrimer **G_2**, λ was switched up to 10 Å and D to 2 m. The corresponding scattering ranges were $0.03 < q < 0.25$ Å^{-1} and $0.01 < q < 0.1$ Å^{-1} respectively, where $q = (4\pi/\lambda)\sin(\theta/2)$ is the scatterring vector and θ the scattering angle.

In the neutron-scattering experiments, four fractions of narrow polydispersity were used for each one of the polymers. For polymer **G_0**, a dozen fractions were obtained manually, by room-pressure gravity-flow SEC in THF through a column (diameter of 3 cm, length of 60 cm) filled with a Bio-Rad-Laboratories gel (Bio-Beads S−X1: molecular-weight separation range of 600−14000); after evaporation of the solvent, these fractions were put together into four fractions of comparable weight. For dendrimers **G_1** and **G_2**, the fractions were obtained by preparative SEC as used in their synthesis. Each fraction was dissolved in perdeuterated tetrahydrofuran (TDF) at a variety of concentrations in the range $0.03 < c < 0.12$ g/mL. The scattering intensity was measured at room temperature in quartz cuvettes (Hellma) with path lengths of 2 mm. The scattering from empty cells and pure solvent, as well as an equivalent incoherent background contribution from the polymer protons, was subtracted as is proper. The scattering intensity was normalized by calibration with an incoherent scatterer (Plexiglas used as a standard), giving the coherent scattered intensity $I(q)$ in absolute units (cm^{-1}) with an accuracy of $\Delta I(q)/I(q) < 2\%$.

The absolute coherent neutron scattering intensity for a monodisperse polymer in dilute solution (where the interparticle structure factor is neglected) may be written as[28,29]

$$I(q) = N_A c\left(\frac{K}{m}\right)^2 M_w P(q) \quad (1)$$

In this equation, N_A is Avogadro's constant and c the concentration of the dissolved polymer (g/mL). Quantity M_w is the weight-average molecular weight of the polymer, and m the molecular weight of the monomer. Quantity $P(q)$ is the z-average form factor. The contrast factor K is given by

$$K = b_m - b_s\frac{v_m}{v_s} \quad (2)$$

In this equation, b_s and b_m are equal to the sum of the scattering lengths of the atoms of one solvent molecule and one monomer repeat unit, respectively, while v_s and v_m are the corresponding specific volumes (1.129 mL/g for TDF, 1.01 mL/g for **G₀**,[30] and ~1 mL/g for **G₁** and **G₂**). The values found for the contrast factor K are -7.79×10^{-12} cm for **G₀**, -7.68×10^{-12} cm for **G₁**, and -7.74×10^{-12} cm for **G₂**, respectively.

In the Guinier small-angle region ($q < q_G$; $q_G = \langle R_g^2\rangle_z^{-1/2}$), the coherent scattering intensity $I(q)$ may be analyzed using the Zimm formula[28,29,31]

$$\frac{c}{I(q)} = \frac{c}{I(0)}\left(1 + \frac{q^2[\langle R_g^2\rangle_z]_c}{3}\right) = \frac{c}{I(0)}\frac{1}{P_c(q)} \quad (3)$$

$$[\langle R_g^2\rangle_z]_c|_{c\to 0} = \langle R_g^2\rangle_z \quad (4)$$

$$\left.\frac{c}{I(0)}\right|_{c\to 0} = \frac{m^2}{N_A M_w K^2} \quad (5)$$

where $\langle R_g^2\rangle_z^{1/2}$ is the z-average radius of gyration of the polymer. After extrapolation to zero concentration (to cancel Viriel interactions), the slope and Y-intercept of the straight line representing the variation of $c/I(q)$ as a function of q^2 permit to determine $\langle R_g^2\rangle_z^{1/2}$ and M_w, respectively.

Beyond the small-angle region ($q > q_G$), the coherent scattering intensity from wormlike polymers may be approximated by Porod−Kratky's formula:[29]

$$P(q) \sim q^{-\gamma} \quad (6)$$

Analysis along this line of the experimental data (if collected in the proper range of q vectors) yields a value for γ and thereby useful structural information on the local properties of the chains and on the conformation and shape of the dendrimer molecules.

III. Results and Discussion

A. Synthesis. The dendrimers studied in the present work were synthesized following the well-known divergent method,[2] which consists of a step by step growth of the molecules through a sequential addition of identical branches starting from a core and proceeding outward. As the branching was chosen to start from a number of sites (the monomer repeating units) along the polymer backbone of a poly(methylhydrosiloxane), the expected dendrimers should be wormlike in shape (see Figure 1). Incidentally, the divergent method also offers a possibility to appreciate in a straightforward manner the role of overcrowding in the branching process and to synthesize homologous generations of dendrimers of a same backbone length, easy to analyze from a conformational point of view.

As shown in Scheme 1, the synthesis was based on the repetition of a hydrosilylation and an alkylation reaction similar to that used previously by others for the preparation of ball-like carbosilane dendrimers.[32−37] The molecular characteristics of the starting **G₀** polymer are given in Table 1. The synthesis of the first generation **G₁** dendrimer consists of applying a platinum-catalyzed hydrosilylation of allyltrichlorosilane with the silane groups of **G₀** to form the intermediate **G₀Cl** product, the chlorosilane groups of which are then reacted with allylmagnesium bromide. The synthesis of the subsequent generations of **G₂**, **G₃**, ... dendrimers is achieved by the hydrosilylation with trichlorosilane of the terminal allyl groups of **G₁**, **G₂**, ... and by the alkylation with allylmagnesium bromide of the terminal chlorosilane groups of the intermediate **G₁Cl**, **G₂Cl**, ... products. After the extractions and washings enumerated in the Experimental Section, dendrimers **G₁**, **G₂**, ... were finally isolated by preparative SEC (Figure 3).

Table 1. Molecular Characteristics of the Starting Polymer G₀ and Synthesized Dendrimers G₁ and G₂

polymer	substitution (%)[a]	M_n[b]	M_w/M_n[b]
G₀		4700	2.8[c]
G₁	100 ± 5	6200	1.2
G₂	84 ± 8	30500	1.6

[a] Average rate of substitution determined by ^{1}H NMR, titration of allylic end groups, and elemental analysis. [b] Number-average molecular weight (in g/mol) and polydispersity determined by SEC in toluene with poly(dimethylsiloxane) standards for **G₀**, and in THF with polystyrene standards for **G₁** and **G₂**. Because of the densely ramified architecture of **G₁** and **G₂**, SEC (calibrated with polystyrene) can only provide a rough value of M_n. [c] Presence of cyclic oligomers (eliminated in **G₁** and **G₂** by preparative SEC).

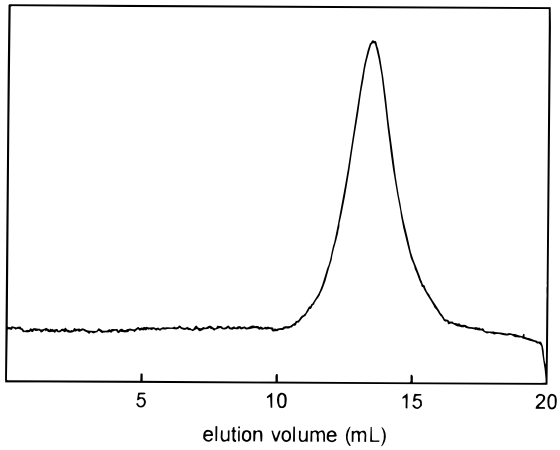

Figure 3. Size-exclusion-chromatography graph of the isolated second-generation **G₂** dendrimer.

Despite their high efficiency, these reactions turned out, however, to be difficult to bring into operation. Because of the slowing down of the reaction kinetics due to an overcrowding of the terminal branches, the use of higher concentrations of catalyst and reagents proved necessary and it proved essential to pursue reactions over longer periods of time in order to reach high rates of substitution. Furthermore, because of a risk of formation of silanol groups (followed by cross-linking of the dendrimers due to a great sensitiveness of the chlorosilane groups to humidity), experiments demanded to be carried out under severe conditions of dryness and in the absence of protic compounds. As an additional precaution, dendrimers **G₁** and **G₂** were submitted to trimethylsilylation[26] as described in the Experimental Section (II.C), to hopefully protect all traces of possibly formed silanol groups. With all these precautions scrupulously taken, dendrimers **G₁** and **G₂** synthesized proved to resist cross-linking over periods of time as long as one or two months. Apparently, infinitesimal traces of silanol groups (undetected by IR

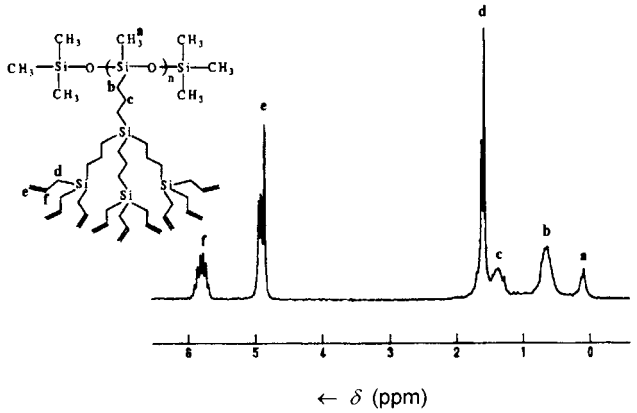

Figure 4. ^{1}H NMR spectrum of the second-generation $\mathbf{G_2}$ dendrimer.

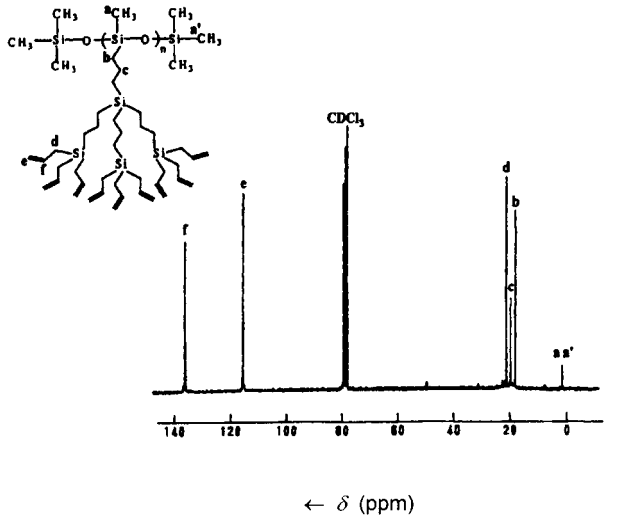

Figure 5. ^{13}C NMR spectrum of the second-generation $\mathbf{G_2}$ dendrimer.

spectroscopy and, at any rate, difficult to measure out experimentally, for instance by ^{29}Si NMR) survived trimethylsilylation. For conscience's sake, the dendrimer samples studied by neutron scattering (see below) were therefore submitted to careful fractionation immediately before use.

The dendrimers $\mathbf{G_1}$ and $\mathbf{G_2}$ synthesized are readily soluble in a wide range of solvents, for instance: THF, toluene, chloroform, or diethyl ether. Their characteristics are summarized in Table 1. According to ^{1}H NMR and chemical titration of double bonds,[27] 100% and 84% of the reactional sites were modified in dendrimers $\mathbf{G_1}$ and $\mathbf{G_2}$, respectively. Quantitative analysis by SEC showed the dendrimers to have a unimodal molecular-weight distribution, and confirmed the absence of coupled molecules and of low-molecular weight impurities. ^{1}H NMR and ^{13}C NMR spectra of dendrimer $\mathbf{G_2}$ are shown in Figures 4 and 5.

Attempts to prepare dendrimer $\mathbf{G_3}$ were unsuccessful. While hydrolyzing the Grignard reagent, a gel was formed at once, before the silanol groups could be protected by trimethylsilylation. Clearly, a large proportion of chlorosilane groups could not participate in the alkylation process, due to steric hindrance and chemical congestion.

As predicted by de Gennes,[3] the step by step growth of dendrimers is limited by overcrowding of the terminal reactive groups and surface congestion. This congestion occurs at a given generation, when the number of end groups becomes so important as to end in a compact arrangement at the outer surface of the dendrimer. The final size of the dendrimer must depend on the number and length of branches as well as on the proper size of the end groups. As already calculated for ball-like dendrimers,[3] the final size of wormlike dendrimers can be evaluated very easily. Proportional to the radius r_i, the outer surface of cylindrically shaped dendrimers increases linearly with the number G_i of successive generations according to the equation

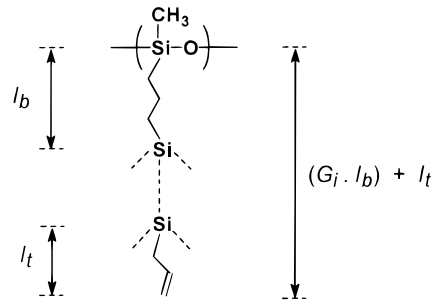

Figure 6. Definition of the branch and dendron lengths used in eq 7.

$$A_D = 2\pi r_i l_m = 2\pi[G_i l_b + l_t] l_m \qquad (7)$$

where A_D represents the extension of the outer surface of the dendrimer molecule (per monomer repeat unit), l_m the spacing of the monomer repeat units along the polymer backbone, l_b the length of the branches in the core of the dendrimer, and l_t the length of the branches sitting on the outer surface (Figure 6). In the same time, the area A_T needed by the end groups of a given monomer unit to arrange at the outer surface increases exponentially according to the equation

$$A_T = N_c N_b^{G_i} A_{vdw} \qquad (8)$$

where N_c and N_b represent the branching multiplicity of the monomer units in the backbone and of the branches themselves, and where A_{vdw} is the cross-sectional area of one terminal group on the outer surface. Sterical congestion arises therefore as soon as A_T increases enough to become equal to A_D. It is quite clear that the shorter the branches and higher the branching multiplicity, the sooner the congestion makes its appearance in the branching process.

In the present work, by choosing $N_c = 1$ and $N_b = 3$, by taking $A_{vdw} = 21$ Å^2 (a typical value for extended hydrocarbon chains[38]), and by deliberately selecting the shortest possible carbosilane branches ($l_m = 2.80$ Å, $l_b = 5.58$ Å, and $l_t = 4.95$ Å, as estimated by molecular modeling with the asumption of full stretching), surface congestion was expected to occur between generations 2 and 3 (Figure 7). It is quite satisfying to note that the chemical congestion observed during the synthesis actually took place at about the second generation. If in fact it occurred somewhat earlier (the rate of substitution of $\mathbf{G_2}$ being of only 84%), it is simply because l_b, l_t, and l_m had been overestimated, the propyl and backbone chains very likely being coiled to some extent.

B. Backbone Conformation. To investigate the role of branching in the backbone conformation of the wormlike dendrimers, the polymers synthesized were submitted to a systematic study by neutron scattering.

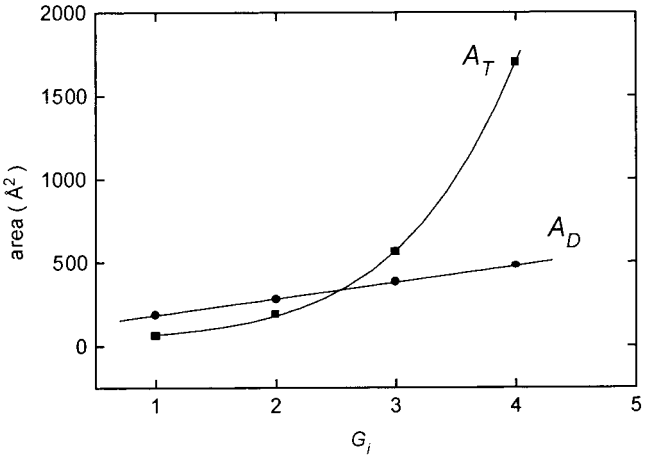

Figure 7. Variation with the number G_i of generations of A_D, available area of the outer surface of the dendrimers, and of A_T, the needed area for the terminal groups, calculated according to eqs 7 and 8.

Table 2. Molecular Characteristics of Fractions of the Starting Polymer G_0 and Synthesized Dendrimers G_1 and G_2

	M_w^{SANS} ± 5−10%[a]	$\langle R_g^2\rangle_z^{1/2}$ ± 5%[a]	M_w/M_n[b]	M_w^{SEC}[b]	L ± 10%[c]	x[d]	$\xi = L/x$ ± 15%[e]
G_0F_1	11700	46.5	1.07	10300	545	42.39	12.9
G_0F_2	9400	42.4	1.09	8200	438	32.65	13.4
G_0F_3	8000	38.8	1.10	7300	373	27.87	13.4
G_0F_4	6200	35.1	1.20	5400	289	19.61	14.7
G_1F_1	28400	55.9	1.10	11700	315	7.245	43.5
G_1F_2	15500	36.5	1.09	7000	172	3.890	44.2
G_1F_3	9400	23.4	1.09	4600	104	3.000	34.7
G_1F_4	7000	18.2	1.07	3300	78	2.310	33.6
G_2F_1	102000	96.0	1.20	65500	403	2.142	(188)
G_2F_2	59900	54.7	1.10	34800	236	2.580	(92)
G_2F_3	41200	38.4	1.10	18300	163	2.355	(69)
G_2F_4	22500	23.1	1.20	10500	89	1.145	(78)

[a] Weight-average molecular weight M_w^{SANS} and z-average radius of gyration $\langle R_g^2\rangle_z^{1/2}$ (in Å) determined by small-angle neutron scattering. [b] Polydispersity M_w/M_n and weight-average molecular weight M_w^{SEC} determined by size-exclusion chromatography in toluene with poly(dimethylsiloxane) standards for **G_0** and in THF with polystyrene standards for **G_1** and **G_2**. [c] Contour length L of the molecules (in Å) deduced from M_w^{SANS} through eq 10. Chain ends were neglected. The length l_m of the monomer repeat units along the backbones was taken to be equal to 2.8 Å and their molecular weights to be equal to 60.13, 252.50, and 709.44 for **G_0**, **G_1**, and **G_2**, respectively. The value of the molecular weight of the **G_2** monomer corresponds to a rate of substitution of 100% instead of 84%. [d] Deduced graphically from eq 11. [e] Persistence length (in Å). Parentheses indicate values deduced with too small values of x for the Benoît−Doty law to be really valid.

This particular technique was chosen in preference to other techniques, such as light or X-ray scattering, because the wavelength of neutrons compares more satisfactorily with the size of the dendrimers under consideration.

For this purpose, the two dendrimers synthesized **G_1** and **G_2** and the starting polymer **G_0** were first fractionated each one into four fractions (noted as **G_iF_j**, $1 \le j \le 4$) as indicated in the Experimental Section (II.D). The molecular weight and molecular-weight distribution of all the fractions were estimated by size-exclusion chromatography calibrated with poly(dimethylsiloxane) standards for **G_0** and polystyrene standards for **G_1** and **G_2** (Table 2). It is important for the interpretation of the neutron-scattering experiments to note that the polydispersities found are very low ($1.07 < M_w/M_n < 1.20$).

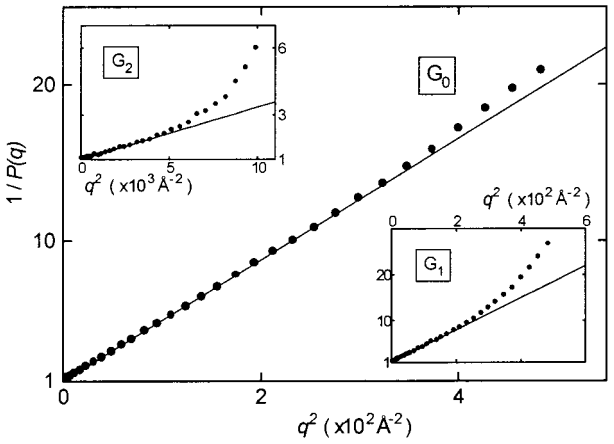

Figure 8. Typical examples of the variation of the reciprocal form factor of the starting polymer **G_0** and of dendrimers **G_1** and **G_2** as a function of the square of the scattering vector, such as determined by small-angle neutron scattering.

The weight-average molecular weight M_w and z-average radius of gyration $\langle R_g^2\rangle_z^{1/2}$ of the **G_iF_j** fractions were then carefully measured by SANS as described in section II-D. Note that, contrary to what happens with dendrimers **G_1** and **G_2**, the M_w values found for the starting polymer **G_0** are in good agreement with those deduced from SEC. The reason is that the hydrodynamic volume of the **G_0** polymer chains is comparable to that of the poly(dimethylsiloxane) standards used in the calibration of the SEC technique. Figure 8 illustrates three typical examples of neutron-scattering curves analyzed in view of determining M_w and $\langle R_g^2\rangle_z^{1/2}$. It is remarkable that, despite the low polydispersity of the fractions investigated, the linear part of the $1/P(q)$ vs q^2 curves extends well beyond the Guinier region (up to about $q_G^* = 7q_G$ for **G_0**, $3q_G$ for **G_1**, and $2q_G$ for **G_2**). The linearity observed for **G_0** cannot be attributed as usual to polydispersity[39] but to the Gaussian shape of the molecules.

The conformation of the polymer chains was assessed from the value of the exponent ν in the power dependence of the radius of gyration upon molecular weight:

$$\langle R_g^2\rangle_z \propto M_w^{2\nu} \tag{9}$$

As is well-known indeed, ν ranges between 0.5 and 0.6 for (Gaussian-excluded volume) threadlike coils and unity for rodlike chains.[40,41] In the present work, the exponent ν deduced from the slope of the straight lines obtained in a doubly logarithmic plot of $\langle R_g^2\rangle_z^{1/2}$ vs M_w (Figure 9), grows very strongly from 0.53 for **G_0** to 0.81 for **G_1** to 0.94 for **G_2**, indicating that the dendrimers gain global rigidity as a function of branching, the conformation going from very flexible for **G_0** to nearly rodlike for **G_2**.

The conformational stretching of the dendrimer molecules as a function of increasing branching is also shown by the growth of the persistence length ξ, which is a statistical quantitative measure of rigidity. For short linear threadlike Gaussian polymers, ξ may be estimated by Benoît-Doty's law:[28,29]

$$\frac{\overline{R_g^2}}{\xi^2} = \frac{x}{3} - 1 + \frac{2}{x} - \frac{2}{x^2}(1 - e^{-x}) \text{ with } x = \frac{L}{\xi} \tag{10}$$

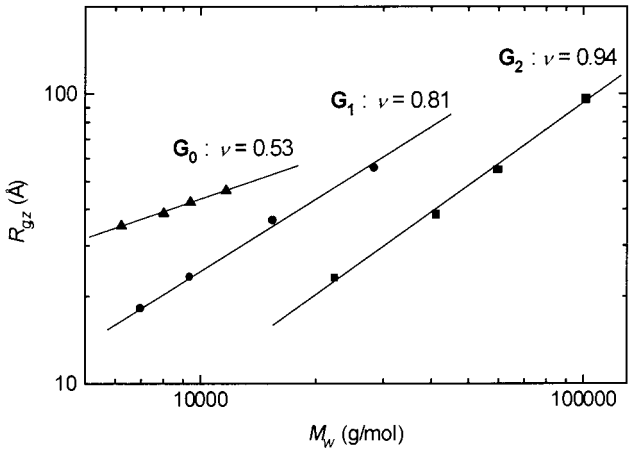

Figure 9. Logarithmic plot of the *z*-average radius of gyration of selected fractions of **G₀**, **G₁**, and **G₂** as a function of the corresponding weight-average molecular weight, as determined by small-angle neutron scattering.

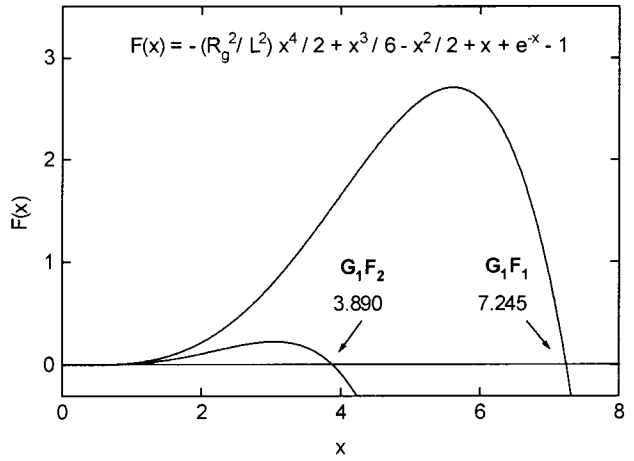

Figure 10. Examples of graphical resolution of eq 12 for fractions **G₁F₂** and **G₁F₁**.

where $\overline{R_g^2}$ represents the mean square radius of gyration and L the contour length of the polymer chains. As expected, this expression simplifies to $\overline{R_g^2} = x\xi^2/3$ when $x \gg 1$, which describes the behavior of flexible Gaussian coils, and to $\overline{R_g^2} = L^2/12$ when $x \ll 1$, which describes the behavior of rodlike particles. For the Benoît-Doty's law to be valid with wormlike chains ($L > \xi$), x has to be significantly greater than unity. According to the theory, ξ values measured through relation 10 increase with L to level off and reach asymptotically their true value at sufficiently high values of L.

As is done in common practice, $\overline{R_g^2}$ was approximated here by the squarre of the *z*-average radius of gyration and L deduced from the weight-average molecular weight M_w using the equation

$$L = \frac{l_m M_w}{m} \qquad (11)$$

where $l_m = 2.8$ Å is the length of the monomer repeat unit along the backbone and m its molecular weight (see Table 2). The persistence length ξ of each one of the fractions was calculated from the experimental data by solving graphically (Figure 10) Benoît-Doty's law, written more conveniently as

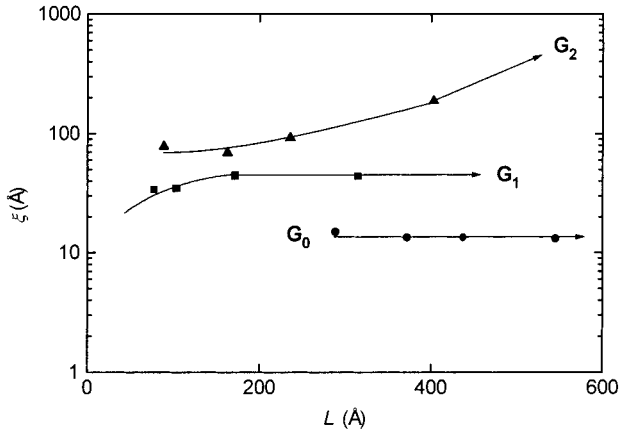

Figure 11. Variation of the calculated persistence length of selected fractions of **G₀**, **G₁**, and **G₂** as a function of the corresponding weight-average contour lengths of the backbones.

$$F(x) = -\frac{1}{2}\frac{\overline{R_g^2}}{L^2}x^4 + \frac{1}{6}x^3 - \frac{1}{2}x^2 + x + e^{-x} - 1 = 0 \qquad (12)$$

The results obtained (Table 2 and Figure 11) show clearly that, in the case of **G₀** where x is sufficiently large ($x > 19$), $\xi \cong 13$ Å is independent of the contour length of the chains and perfectly consistent with the classical values found in the literature for flexible polymers.[42] For **G₁** where x is moderately large ($2 < x < 7$), ξ levels off rapidly as a function of increasing x to reach a value close to 44 Å. Finally, for **G₂** where x is small ($x < 3$), ξ grows steadily up to about 200 Å without ever reaching an asymptotic value. On the whole, ξ increases significantly from 13 Å for **G₀** to 44 Å for **G₁** to over 200 Å for **G₂**, that is, to a value not far from the average contour length of the molecules. This demonstrates beyond any discussion the dramatic effect of steric hindrance on the conformation of the dendrimer molecules. Despite the high flexibility of the polysiloxane backbones and propylsilane branches, the dendrimer molecules stretch out upon branching considerably, so much as to extend almost to full length for **G₂** Equation 7 helps us understand this behavior. Indeed, to relax the overcrowding of the terminal groups brought about by branching, it is enough to increase the outer surface of the dendrimer molecules, that is, their radius and their overall length by stretching branches and backbones.

The main concern of the present work was to appreciate the conformational change of the dendrimers as a function of increasing branching density. The approach deliberately chosen was to analyze the molecular-weight dependence of the radius of gyration of the **G₀**, **G₁**, and **G₂** polymers, by fractionating the polymers into several fractions of low polydispersity and studying separately each one of the fractions by SANS in the Guinier region ($q < q_G$). In principle, a rough estimate of the persistence length, along with further information about the macroscopic shape and microscopic structure of the macromolecules may be gained by analyzing the scattering curves beyond the Guinier region. Indeed, according to Porod and Kratky,[29] the scattering intensity at $q > q_G$ varies as $I(q) \sim q^{-\gamma}$ and its examination permits to determine γ and $q^* \approx 2\pi/d^* = \pi/\xi$. The q^* value corresponds to a crossover between two regimes: for $q_G^* < q < q^*$, the exponent γ depends essentially on the global shape of the molecules (it is equal to 1 for thin

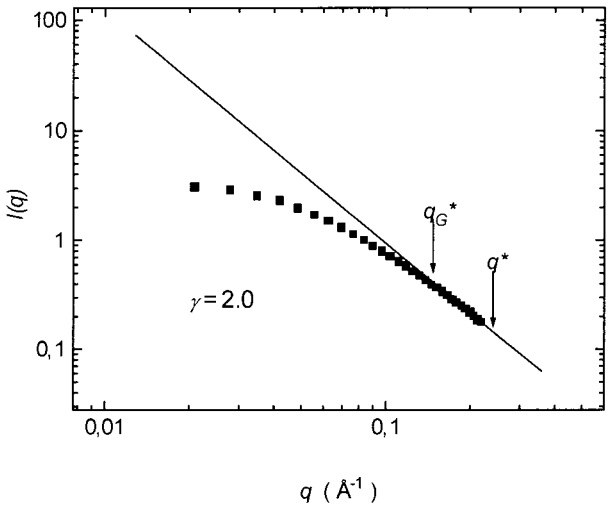

Figure 12. Shape of the neutron scattering curve of fraction $\mathbf{G_0F_1}$. Arrows indicate the limit q_G^* of the observed linear Guinier behavior and the limit q^* of the intermediate range of scattering vectors. The straight line provides a value for exponent γ in eq 6.

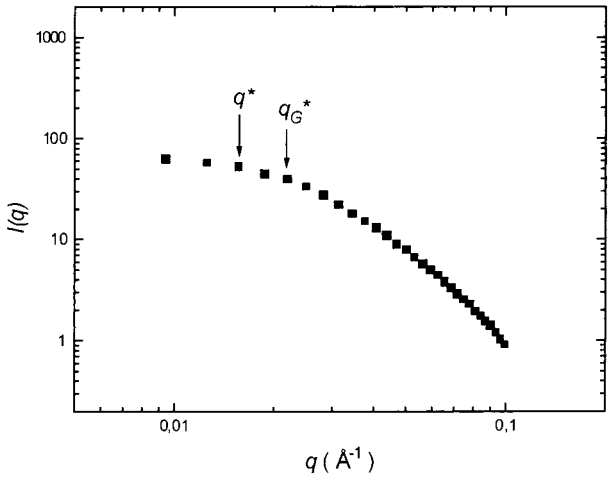

Figure 13. Shape of the neutron scattering curve of fraction $\mathbf{G_2F_2}$. Arrows indicate the limit q_G^* of the observed linear Guinier behavior and the limit q^* of the intermediate range of scattering vectors. The hidden intermediate regime does permit one to calculate a value for exponent γ in eq 6.

rods, to 2 for flexible coils, and to 4 for particles with sharp interfaces), while, for $q > q^*$, it depends on the interactions between polymer and solvent molecules (it is equal to 2 in bad solvents and to about 1.7 in good solvents). In the present work, the $q > q^*$ region could not be analyzed satisfactorily because, under the experimental conditions used, the intensity measurements were not sufficiently accurate. As for the intermediate $q_G^* < q < q^*$ region, it turned out sufficiently wide for $\mathbf{G_0}$ (Figure 12), very narrow for $\mathbf{G_1}$, and nonexistent for $\mathbf{G_2}$ (Figure 13). It was thus possible to determine γ safely in the case of $\mathbf{G_0}$ alone; the value found, $\gamma = 2.0$, indicates clearly that this polymer has a Gaussian random-coil conformation as expected. The value, $\gamma \approx 1.4$, tentatively estimated for $\mathbf{G_1}$, suggests for this polymer a conformation lying between rodlike and random coil. A comprehensive picture of the results obtained by neutron scattering is summarized in Table 3.

C. Thermal and Structural Properties. Before discussing the thermal and structural properties of the

Table 3. Conformational Characteristics of the Starting Polymer G_0 and Synthesized Dendrimers G_1 and G_2 as Deduced from Small-Angle Neutron Scattering

polymers	ν^a	ξ (Å)^b	γ^c
$\mathbf{G_0}$	0.53	13	2.0
$\mathbf{G_1}$	0.80	44	≈1.4
$\mathbf{G_2}$	0.94	>200	

[a] Exponent in eq 9. [b] Persistence length deduced graphically through eq 12. [c] Exponent in eq 6.

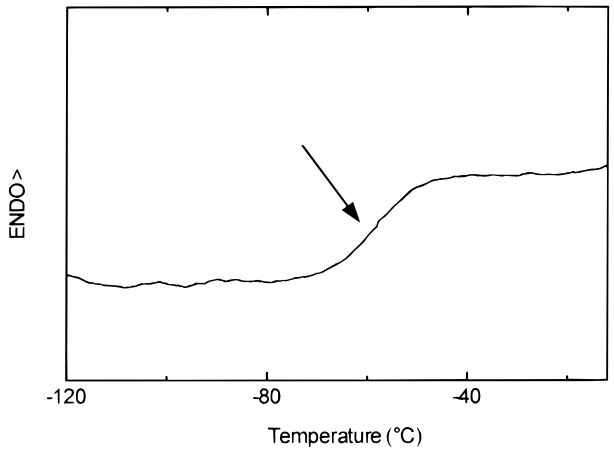

Figure 14. Differential-scanning-calorimetry thermogram of $\mathbf{G_2}$. The arrow (at the inflection point) indicates the presence of a glass transition.

dendrimers synthesized, it is worth noting that, on proceeding from the starting poly(methylhydrosiloxane) $\mathbf{G_0}$ to the second generation dendrimer $\mathbf{G_2}$, the bulk viscosity increases dramatically. While $\mathbf{G_0}$ is very fluid, $\mathbf{G_1}$ is already quite viscous and $\mathbf{G_2}$ is just as hard as a waxy paste. This behavior results, of course, from the increasing rigidification of the backbone conformation. To check if, by any chance, such an important rigidification were able also to induce liquid crystallinity, the dendrimers were subjected to a careful examination by polarizing optical microscopy and X-ray diffraction. The conclusion was straightforward. Not only $\mathbf{G_1}$ but also the more densely crowded $\mathbf{G_2}$ showed no sign of optical birefringence or of spontaneous ordering above room temperature, not even the slightest tendency to orientation in strong magnetic fields. To make sure that liquid crystals would not eventually form at low temperatures, the dendrimers were also subjected to differential scanning calorimetry. But the thermograms recorded between −170 and +50 °C did not show the presence of any first-order phase transition. The samples were simply undergoing a (single) glass transition as shown in Figure 14. The glass transition temperatures, measured at the inflection point of the thermograms, were found to grow considerably with branching, from −144 °C for $\mathbf{G_0}$ to −94 °C for $\mathbf{G_1}$ to −68 °C for $\mathbf{G_2}$. In agreement with the observed increase in viscosity, this behavior is clearly related to the stiffening of the polymer backbones.

Conclusion

Two generations of wormlike dendrimers made of purely flexible and noninteracting segments were synthesized. These consisted of a polysiloxane backbone carrying carbosilane dendrons on every monomer unit. Using a divergent approach, the synthesis was conducted by a stepwise chemical modification of a poly-

(methylhydrosiloxane) through alternating sequences of hydrosilylation and alkylation reactions. To run the reactions close to completion, and to avoid chain scission and parasitic coupling reactions, an elaborate synthetic procedure was worked out, fixing the appropriate experimental conditions (catalyst and reagents concentrations, temperature, duration of reactions, use of neutral and rigorously anhydrous media). By using short propylsilane branches, chemical congestion was obtained at the second generation as expected on geometrical grounds. As determined by ^{1}H NMR, chemical titration of the allylic end groups, and elemental analysis, the rate of substitution of the carbosilane dendrons on the polymer backbone was found to be 100% for $\mathbf{G_1}$ and 84% for $\mathbf{G_2}$.

Small-angle neutron-scattering experiments, performed on dilute solutions of well-defined fractions of $\mathbf{G_0}$, $\mathbf{G_1}$, and $\mathbf{G_2}$, showed that the backbones of the polymers were stretching out considerably upon branching, going from a Gaussian random conformation for $\mathbf{G_0}$ to an almost fully extended rodlike conformation for $\mathbf{G_2}$. Considering that the constituent parts of the dendrimers are intrinsically flexible, the conformational stretching observed can only be attributed to an overcrowding of the branches at the periphery.

Finally, optical observations with a polarizing microscope and X-ray diffraction experiments showed, contrary to all expectations, that the dendrimers were perfectly isotropic and amorphous. Even though fully stretched, the molecules—even those of $\mathbf{G_2}$—revealed incapable of spontaneously orienting themselves parallel to one another and thus of producing nematic or columnar liquid crystals. This is probably due to their dynamical flexibility, the persistence time of their stretched conformations being, to all appearances, too short for the anisotropic interactions to develop efficiently over macroscopic distances.

Acknowledgment. We express our gratefulness to Prof. H. Benoît, and to Drs. G. Friedmann, C. Picot, and M. Rawiso for fruitful discussions.

References and Notes

(1) Tomalia, D. A.; Naylor, A. M.; Goddard, W. A., III. *Angew. Chem., Int. Ed. Engl.* **1990**, *29*, 138.
(2) Newkome, G. R.; Moorefield, C. N.; Vögtle, F. *Dendritic Molecules: Concepts, Syntheses, Perspectives*; VCH: Weinheim, Germany, 1996.
(3) de Gennes, P. G.; Hervet, H. *J. Phys. (Paris)* **1983**, *44*, L351.
(4) For a review, see: Frey, H. *Angew. Chem., Int. Ed. Engl.* **1998**, *37*, 2193.
(5) Tomalia, D. A.; Kirchoff, P. M. U.S. Pat. 1987, 4 694 064.
(6) Yin, R.; Zhu, Y.; Tomalia, D. A. *J. Am. Chem. Soc.* **1998**, *120*, 2678.
(7) Karakaya, B.; Claussen, W.; Shäfer, A.; Lehmann, A.; Schlüter, A. D. *Acta Polym.* **1996**, *47*, 79.
(8) Karakaya, B.; Claussen, W.; Gessler, K.; Saenger, W.; Schlüter, A.-D. *J. Am. Chem. Soc.* **1997**, *119*, 3296.
(9) Klopsch, R.; Franke, P.; Schlüter, A. D. *Chem.—Eur. J.* **1996**, *2*, 1330.
(10) Freudenberger, R.; Claussen, W.; Schlüter, A. D.; Wallmeier, H. *Polymer* **1994**, *35*, 21.
(11) Neubert, I.; Amoulong-Kirstein, E.; Schlüter, A. D.; Dautzenberg, H. *Macromol. Rapid Commun.* **1996**, *17*, 517.
(12) A styrene-based copolymer with about 1.5% of repeat units bearing dendrons up to the fourth generation has been reported by: Hawker, C. J.; Fréchet, J. M. J. *Polymer* **1992**, *33*, 1507.
(13) Chen, Y. M.; Chen, C. F.; Lu, W. H.; Li, Y. F.; Xi, F. *Macromol. Rapid Commun.* **1996**, *17*, 401.
(14) Draheim, G.; Ritter, H. *Macromol. Chem. Phys.* **1995**, *196*, 2211.
(15) Kaneko, T.; Horie, T.; Asano, M.; Aoki, T.; Oikawa, E. *Macromolecules* **1997**, *30*, 3118.
(16) (a) Percec, V.; Heck, J.; Tomazos, D.; Falkenberg, F.; Blackwell, H.; Ungar, G. *J. Chem. Soc., Perkin Trans.* **1993**, *1*, 5. (b) Percec, V.; Schlueter, D. *Macromolecules* **1997**, *30*, 5783 and references therein.
(17) Percec, V.; Ahn, C. H.; Ungar, G.; Yeardley, D. J. P.; Möller, M.; Sheiko, S. S. *Nature* **1998**, *391*, 161.
(18) Claussen, W.; Schulte, N.; Schlüter, A. D. *Macromol. Rapid Commun.* **1995**, *16*, 89.
(19) Stewart, G. M.; Fox, M. A. *Chem. Mater.* **1998**, *10*, 860.
(20) Jahromi, S.; Palmen, J. H. M.; Steeman, P. A. M. *Macromolecules*, **2000**, *33*, 577.
(21) Zhishan, B.; Rabe, J. P.; Schlüter, A. D. *Angew. Chem., Int. Ed. Engl.* **1999**, *38*, 2370.
(22) Prokhorova, S. A.; Sheiko, S. S.; Möller, M.; Anh, C. H.; Percec, V. *Macromol. Rapid Commun.* **1998**, *19*, 359.
(23) Stocker, W.; Schürmann, B. L.; Rabe, J. P.; Förster, S.; Lindner, P.; Neubert, I.; Schlüter, A. D. *Adv. Mater.* **1998**, *10*, 10.
(24) Stocker, W.; Karakaya, B.; Schürmann, B. L.; Rabe, J. P.; Schlüter, A. D. *J. Am. Chem. Soc.* **1998**, *120*, 7691.
(25) Forster, S.; Neubert, I.; Schlüter, A. D.; Lindner, P. *Macromolecules* **1999**, *32*, 4043.
(26) Sweeley, C. C.; Bentley, R.; Makita, M.; Wells, W. W. *J. Am. Chem. Soc.* **1963**, *85*, 2497.
(27) Chemical titration of the −C═C− according to: Johnson, J. B.; Fletcher, J. P. *Anal. Chem.* **1959**, *31*, 1663.
(28) Benoît, H.; Doty, P. *J. Phys. Chem.* **1953**, *57*, 958.
(29) Benoît, H.; Higgins, J. S. In *Polymers and Neutron Scattering*; Clarendon Press: Oxford, England, 1994.
(30) *Silicones and Silicon-containing polymers*; Petrarch Inc. catalogue 1994−95; p 24.
(31) Guinier, A.; Fournet, G. *Small Angle Scattering of X-rays*, John Wiley and Sons: London, 1955.
(32) Friedmann, G. Unpublished results.
(33) van der Made, A. W.; van Leeuwen, P. W. N. M. *J. Chem. Soc., Chem. Commun.* **1992**, 1439.
(34) Zhou, L. L.; Roovers, J. *Macromolecules* **1993**, *26*, 963.
(35) Seyferth, D.; Son, D. Y.; Rheingold, A. L.; Ostrander, R. L. *Organometallics* **1994**, *13*, 2682.
(36) Kim, C.; Park, E.; Jung, I. *J. Korean Chem. Soc.* **1996**, *40*, 347.
(37) Lorenz, K.; Mulhaupt, R.; Frey, H.; Rapp, U.; Mayer-Posner F. J. *Macromolecules* **1995**, *28*, 6657.
(38) (a) Doolittle, A. K. *J. Appl. Phys.* **1951**, *22*, 1471. (b) Donnio, B.; Heinrich, B.; Gulik-Grzywicki, T.; Delacroix, H.; Guillon, D.; Bruce, D. W. *Chem. Mater.* **1997**, *9*, 2951.
(39) Rawiso, M. *J. Phys. IV Fr.* **1999**, *9*, Pr1.
(40) Oberthür, R. C. *Makromol. Chem.* **1978**, *179*, 2693.
(41) Tanford, C. *Physical Chemistry of Macromolecules*; John Wiley and Sons: New York, 1961.
(42) Brandrup, J.; Immergut, E. H. In *Polymer Handbook*, 3rd ed.; Wiley-Interscience: New York, 1989.

MA000327K